3D numerical investigation of mechanized twin tunnels in soft ground - Influence of lagging distance between two tunnel faces

3D Numerical Investigation of Mechanized Twin Tunnels in Soft Ground – Influence of Lagging Distance between Two Tunnel Faces

Ngoc-Anh Do[1], Daniel Dias[2], Pierpaolo Oreste[3]
[1]Hanoi University of Mining and Geology, Faculty of Civil Engineering, Department of Underground and Mining Construction, Hanoi, Vietnam
[2]Grenoble Alpes University, Laboratory 3SR, Grenoble, France
[3]Politecnico di Torino, Department of Environmental, Land and Infrastructural Engineering, Italy

Abstract:
During the construction of twin mechanized tunnels, a large impact of lagging distance is expected due to the strong effects of external loads and also the time dependence of the tunnel behaviour along the direction of tunnelling. Most researches in the literature focused on the influence of the distance between the tunnels' axis and their relative position. In this study, a 3D numerical investigation was carried out of the interaction between twin mechanized tunnels excavated in a horizontally parallel section. Special attention was paid to the influence of the lagging distance between the two mechanized tunnel faces. The numerical results indicated that the critical situation in terms of the lining stability occurs when the face of the following tunnel is at the same transverse section as the preceding tunnel. The tendency in the change of the bending moment and the lining deformation in the preceding tunnel and the following tunnel are generally opposite, depending on the lagging distance.

Keywords: *Numerical modelling; Lining response; Segmental lining; Settlement; Lagging distance; Twin tunnel.*

1. Introduction

During excavation of tunnels close to each other, significant interactions between tunnels have been presented in the literature. A review of twin tunnel interaction has been given in recent works by the authors of the present work [1-4]. Accordingly, most researches have focused on the interaction between two horizontally driven tunnels using physical tests [5-7], empirical/analytical methods [8,9], field measurements [8-14], and numerical analyses [15-22]. They considered the interaction between twin tunnel in terms of the ground deformation, but not the structural forces induced in tunnel linings [2].The effect of the tunnel location in transverse section, i.e. tunnel distance or different depths of tunnels, etc., was thoroughly studied. However, less work has been devoted to the influence of lagging distance, along the tunnel advance direction, between tunnel faces on the change in structural forces, lining deformation and ground displacement.

Tunnels can nowadays be excavated using conventional methods such as the New Austrian Tunnelling Method (NATM) or mechanized methods such as shield machines, tunnel boring machines, pipe jacking, and so on. While NATM tunnels are mainly supported by shotcrete, rock bolts and steel ribs, a mechanized tunnel is however usually excavated using a shield machine, supported by segmental concrete lining. NATM method can be used in tunnel with arbitrary shape but mechanized tunnel is usually applied for circular tunnels. Then, the behaviour of twin NATM tunnels and that of twin mechanized tunnels excavated in the same condition are therefore not similar.

Ng. et al. [22] presented an interesting numerical investigation on the multiple interactions between large parallel hypothetical twin tunnels constructed in stiff soils using the NATM. This study pays special attention to the influence of the lagging distance between twin tunnel excavated faces (L_F), indicating a strong effect of L_F on the behaviour of both tunnels. It should be mentioned that the behaviour of tunnels excavated using the NATM method and the mechanized method are very different, caused not only by the tunnel shape but also by the components of the construction loading along the tunnelling direction.

Along the axis of the tunnel excavated using the mechanized method, there are some construction loads such as slurry/mud pressures on the tunnel face, jacking forces and compensation grouting pressures at the shield tail and so on. These forces have a strong effect on the behaviour of a single tunnel, not only in terms of structural forces and lining deformation, but also on the displacement of the ground surrounding the tunnel [22]. Generally, under the impact of jacking forces and grouting pressure, the greatest normal forces and longitudinal forces induced in a lining ring are reached right after their installation behind the shield tail. These two structural forces then gradually decrease as the grout hardens and the shield machine advances further away from the measured lining section. However, their values increase again due to a gradual increase in ground loads. The steady state of the tunnel lining is only reached after a tunnel advance of about $5D_{tu}$ (D_{tu} is external diameter of the tunnel).

Evidently, each of above loading components in the mechanized tunnelling method has only a certain impact range in the transverse section and also along the tunnelling direction. During the excavation of twin mechanized tunnels, the interaction between two tunnels therefore depends on both their distance and relative location in transverse section, and the lagging distance between the two tunnel faces along the tunnelling direction. Do et al. [3] conducted a series of tridimensional (3D) numerical analyses, which showed that tunnel distance had a great effect on the interaction between two tunnels. In this study, the following tunnel is excavated when the preceding tunnel has reached a steady state.

Also, using 3D numerical models of twin horizontal mechanized tunnels, Do et al. [2] focused on the effect of the tunnelling procedure in which the two tunnels are simultaneously excavated (case 1) and successively excavated when the preceding tunnel has reached a steady state before the excavation of the following tunnel (case 2). The numerical results indicated that the simultaneous excavation of twin tunnels causes smaller structural forces and lining displacement than those induced in the case of twin tunnels that are successively excavated. However, the simultaneous excavation of twin tunnels can result in a greater settlement above the two tunnels.

A detailed investigation of the influence of the lagging distance between tunnel faces on their interaction has not yet been conducted in any of the above studies. Obviously, due to the strong effects of external loads along the tunnelling direction in mechanized tunnelling and also the time dependence of the tunnel behaviour, the lagging distance can be expected to have a great impact; thus, this is the goal of the present study. A 3D numerical investigation of the interaction between twin mechanized tunnels (with varying lagging distance), using the $FLAC^{3D}$ finite difference code [23] has been carried out. The numerical results presented in section 3 indicate that the critical situation in terms of the lining stability is when the face of the following tunnel is at the same transverse section as the shield tail of the preceding tunnel. The changes in structural forces, deformation of the tunnel linings and the displacement of the ground surrounding the tunnel, which are caused by the effect of the lagging distance, have been highlighted.

2. Numerical model

Figures 1 and 2 show a plan view and a cross section of the 3D model used in this study. Basically, the same 3D numerical model developed in the finite difference program FLAC^{3D} [23] used in another work by the same authors [2,3] has been adopted in the present study. All the parameters used in the numerical model are the same as those applied in previous works by Do et al. [2,24,25]. Therefore, only a short description is given here.

2.1. Soil's constitutive model

The parameters from the Bologna-Florence high speed railway line project in Italy have been adopted for use in this study. The soil has been modelled using the Cap-Yield (CYsoil) constitutive model, which is a strain-hardening constitutive modelthat is characterized by a frictional Mohr-Coulomb shear envelope (zero cohesion) and an elliptic volumetric cap in the (*p', q*) plane [23,24]. Parameters of the soil are shown in Table 1 [4,24].

Table 1. Parameters of the soil [4,24]

CYsoil model	Value
Reference elastic tangent shear modulus G^e_{ref} (MPa)	58
Elastic tangent shear modulus G^e (MPa) $G^e = G^e_{ref}\left(\sigma_3 / p^{ref}\right)$	98
Elastic tangent bulk modulus K^e (MPa) $K^e = K^e_{ref}\left(\sigma_3 / p^{ref}\right)$	213
Reference effective pressure p^{ref} (kPa)	100
Failure ratio R_f	0.9
Ultimate friction angle ϕ_f (degrees)	37
Calibration factor β	2.35
Lateral earth pressure factor K_0	0.5

2.2. Shield machine simulation

The twin horizontal tunnels are excavated at a space distance of 11.75 m from centre to centre. The tunnels have an external excavation diameter including the lining thickness (D_{tu}) of 9.4m and were excavated at a depth of 20 m below the ground surface.

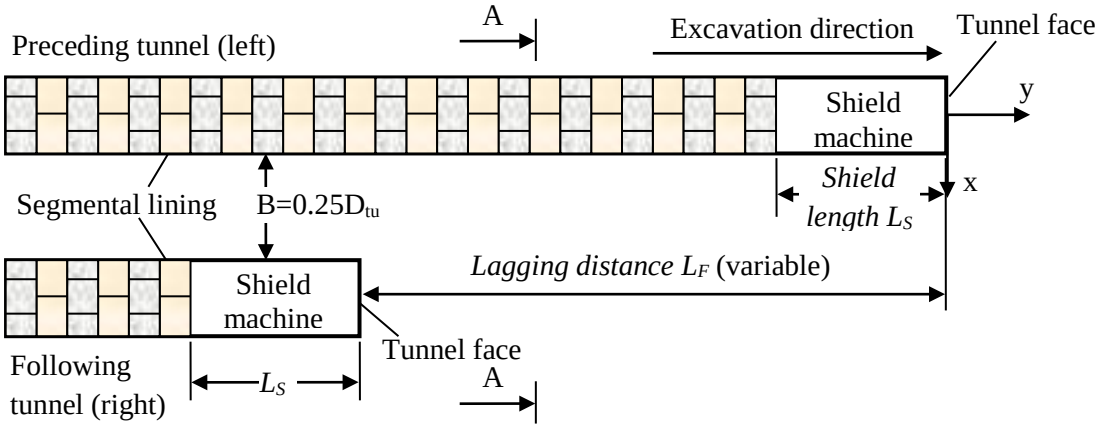

Figure 1. Plan view of the twin tunnels (not scaled) (from Do et al. [2])

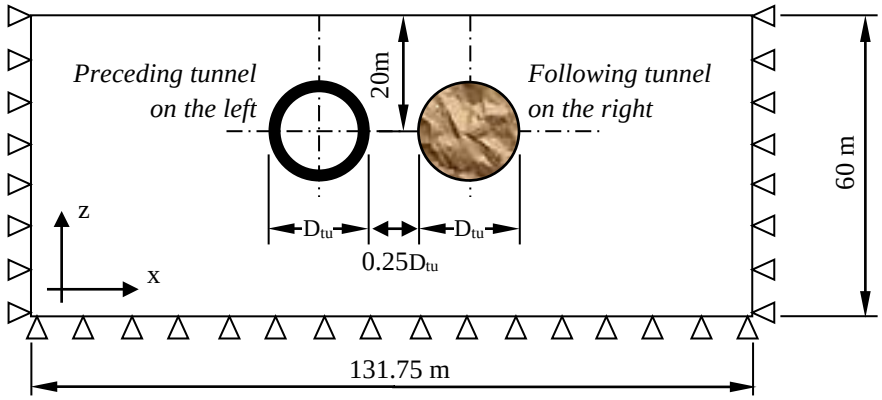

Figure 2. A–A: typical cross section view of the twin tunnels (not scaled) (from Do et al. [2])

The tunnel construction process has been modelled using a step-by-step approach [24]. The advance length of 1.5 m after each excavation has been used, which is equal to the width of a lining ring. A schematic view of the present shield machine is provided in Figure 3.

In this 3D numerical model, most components of a shield machine have been simulated: trapezoidal distribution pressure applied from the shield chamber to the tunnel face, distribution pressure applied to the ground surface in the cylindrical void just behind the tunnel face, the shield machine and its conicity, the self-weight of the shield machine, the jacking force at the shield tail, the grouting pressure in the liquid state and the hardened grout, the tunnel linings with the joints and the back-up train(see Figure 3).

Detailed descriptions of the numerical simulation of each of the above components can be seen in the work by the same authors [2,24] and these are therefore not described here again. It should be noted that the presence of the joints in the tunnel lining, including the longitudinal joints and the circumferential joints, has been taken into consideration in this model due to their important influence [26]. The parameters of the tunnel lining are indicated in Table 2 [2,4,24].

Table 2. Lining parameters [2,4,24]

Parameter	Symbol	Value	Parameter	Symbol	Value
Young's modulus (GPa)	E_l	35	Rotational stiffness (MN.m/rad/m)	K_θ	100
Poisson's ratio	ν_l	0.15	Axial stiffness (MN/m)	K_A	500
Lining thickness (m)	t_l	0.4	Radial stiffness (MN/m)	K_R	1050
External diameter (m)	D_{tu}	9.4	Rotational stiffness (MN.m/rad/m)	$K_{\theta R}$	100
Concrete lining density (kN/m)	γ	23	Axial stiffness (MN/m)	K_{AR}	500
Width of lining ring (m)	w	1.5	Radial stiffness (MN/m)	K_{RR}	1050

The longitudinal joints between segments in a lining ring were simulated by a set composed of a rotational spring (K_θ), an axial spring (K_A) and a radial spring (K_R) [2,3,24]. Similarly, the rigidity characteristics of the circumferential joint between the successive lining rings were represented by a set composed of a rotational spring ($K_{\theta R}$), an axial spring (K_{AR}) and a radial spring (K_{RR}) (see Table 2).

In order to show the effect of the lagging distance L_F, the excavation process of the twin tunnels has been modelled as follows: (i) excavation of the preceding tunnel (left); (ii) excavation of the following tunnel (right) at a certain lagging distance L_F behind the face of the preceding tunnel. Five scenarios of the lagging distance L_F were simulated: $0L_S$, $1L_S$, $2L_S$, $3L_S$ and $8L_S$, in which L_S is the length of the shield machine (L_S=12 m). These lagging distances correspond to the cases $0D_{tu}$, $1.25D_{tu}$, $2.55D_{tu}$, $3.8D_{tu}$ and $10D_{tu}$, where D_{tu} is the external diameter of the tunnel. The case $L_F = 0\ L_S$ means that the two tunnels are being simultaneously excavated, while the value $L_F = 1\ L_S$ corresponds to the situation that the face of the following tunnel is at the same transverse section as the shield tail of the preceding tunnel. The case $L_F = 8\ L_S$ implies that the following tunnel is excavated at a distance behind the preceding tunnel, which is large enough so that the structural forces in the preceding tunnel lining have reached the steady state. All the numerical calculations were conducted without considering the presence of underground water.

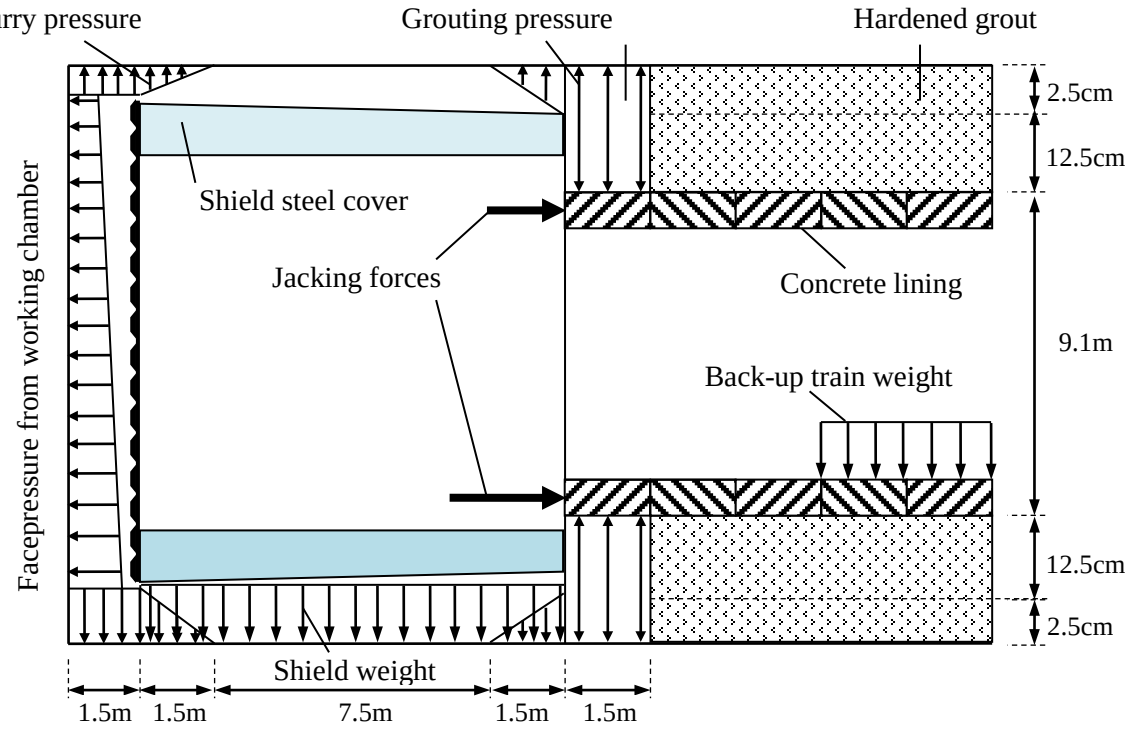

Figure 3. Layout of the shield machine model (not scaled) (from Do et al. [24]).

3. Numerical results and discussion

This section deals with the variations of the structural forces induced in the tunnel linings and the ground displacements developed over the tunnels during the excavation of the parallel tunnels at different lagging distances, L_F. These variations were determined at the section of the 30th ring, counting from the model boundary (y = 0 m) when the tunnel excavation reached a steady state. The influence of the boundary condition on tunnel behaviour is negligible at this section [2,24].

3.1. Surface settlement and lining deformation

Figure 4shows the surface settlement troughs developed over twin tunnels excavated at different lagging distances between the faces of the two tunnels. For ease of comparison, the

settlement trough over a single tunnel is also presented. The great influence of the lagging distance between the tunnel faces on the ground deformation can be seen in this figure. The greatest surface settlement is observed when the two mechanized tunnels are simultaneously excavated, that is, the lagging distance is zero. The settlement trough is symmetrical over the twin tunnels. The increase in the lagging distance (i.e. $L_F = 1L_S$, $2L_S$, $3L_S$) causes a decrease in the maximum surface settlement (also see Table 3). The shape of the settlement trough is still more or less symmetrical over the tunnels. However, when the lagging distance is large enough (i.e. $L_F = 8L_S$), an increase of the surface settlement trough over the twin mechanized tunnels is again observed and the maximum value of the settlement moves toward the tunnel which is first excavated. The increase of the maximum surface settlement and the change in shape of the surface settlement trough when the two tunnels are simultaneously excavated compared to the case of the large lagging distance $L_F = 8L_S$ has been discussed by the same authors [2]. In the latter case, a gradual movement of the surface settlement trough from the preceding tunnel to the following tunnel is expected and the maximum surface settlement is inclined to the preceding tunnel. However, the results obtained in this study for other cases when the lagging distance between the tunnel faces is small (i.e. $L_F = 1L_S$, $2L_S$, $3L_S$) show a nearly symmetrical surface settlement trough over the twin tunnels.

Based on the volume loss ratios presented in Table 4, which is related to surface deformation developed above twin tunnels, it can be seen that the additional volume loss ratio caused by the excavation of the following tunnel in all cases of investigated lagging distances between two tunnel faces is smaller than the one caused by the excavation of the single preceding tunnel (0.92%). This observation is also supported by the development of plastic zones around each tunnel as can be seen in Figure 5. Accordingly, the size of the plastic zones around the following tunnel is smaller compared to the one developed around the preceding tunnel. The same observation of smaller surface settlements developed above the following tunnel was also obtained from the field measurement introduced by Suwansawat and Einstein [8], Chen et al. [11]. The above volume loss ratio results induced by the second tunnel (see Tables 3, 4) are however different from laboratory and numerical results obtained by Chapman et al. [5] and Addenbrooke and Potts [27]. Their work showed a larger volume loss ratio caused by the excavation of the second tunnel. This difference could be attributed to the clayey nature of their soils or due to the undrained behaviour taken into consideration in their researches. These conditions are not similar to those in the present study (sandy soil and no underground water).

It is also interesting to note that the higher the lagging distance is, the smaller the additional volume loss ratio and the total volume loss ratio will be above twin tunnels at the steady state (see Table 4).

This phenomenon can be explained by the fact that when the lagging distance L_F is large enough, the following tunnel is excavated when the surface settlement trough over the single preceding tunnel has reached a steady state. The excavation of the following tunnel causes large lateral movements of the soil in the zone between the two tunnels toward the following tunnel, and is followed by large downward movements of the soil above the preceding tunnel, as can be seen from the normal displacements presented in Figure 6 and Table 3. On the other hand, the downward movement over the following tunnel in this case is small compared to the other investigated cases. This could be because the following tunnel is excavated through a soil zone which was disturbed by the excavation of the preceding tunnel. Consequently, a certain movement of the soil above the following tunnel has taken place before the excavation of the following tunnel, and the rest of the downward movement over this new tunnel is therefore reduced, as can be seen in Figure 7 and Table 4.

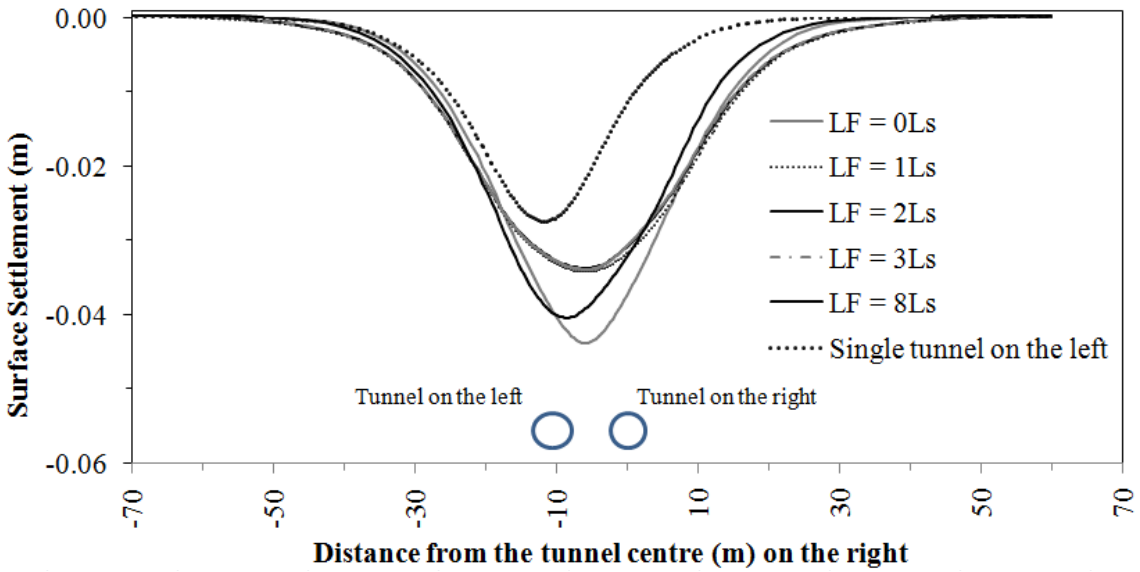

Figure 4. Comparison of the surface settlement troughs in the transverse section of the twin lagging tunnels (L_F is the lagging distance between tunnels faces, L_S is the length of the shield machine).

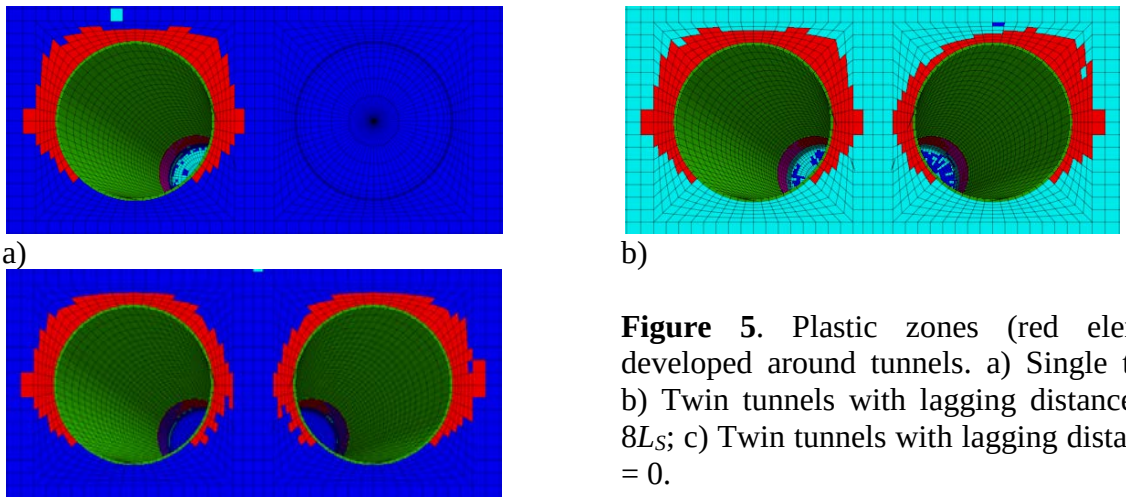

a) b)

c)

Figure 5. Plastic zones (red elements) developed around tunnels. a) Single tunnel; b) Twin tunnels with lagging distance L_F = $8L_S$; c) Twin tunnels with lagging distance L_F = 0.

As for the lining deformation which is also related to the movement of the soil, when the lagging distance between the two tunnel faces decreases, the downward movements developed in the lining the preceding tunnel at the final state also decrease compared the case of a large lagging distance (see Figure 6 and Table 3). On the other hand, the downward movement that develops in the lining the following tunnel increases when the lagging distance decreases (see Figure 7 and Table 4). The decrease in the difference between the downward movement over the two tunnels when the lagging distance decreases (i.e. L_F = $1L_S$, $2L_S$, $3L_S$) is the reason for the nearly symmetrical shape of the settlement trough over twin tunnels (see Figure 4).

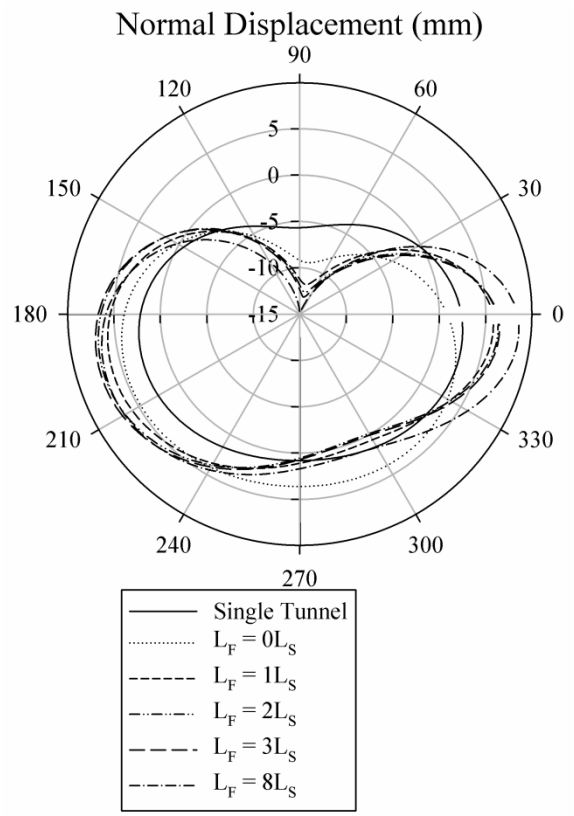

Figure 6. Normal displacement induced in the lining of the preceding tunnel on the left.

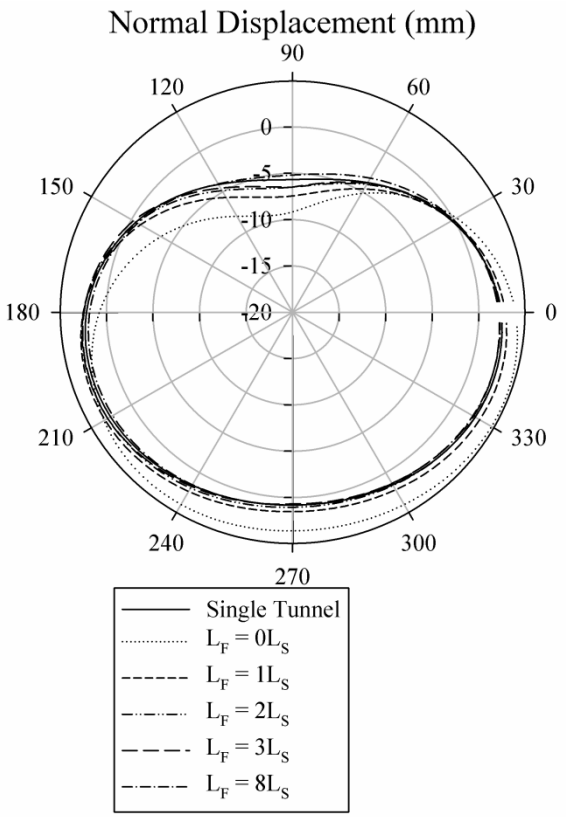

Figure 7. Normal displacement induced in the lining of the following tunnel on the right.

3.2. Normal forces and longitudinal forces in the tunnel lining

Figures 8 and 9 show a significant effect of the lagging distance between tunnel faces on the normal forces induced in the preceding tunnel on the left and the following tunnel on the right at the steady state. The excavation of twin mechanized tunnels always causes an increase in the normal forces induced in the lining of both the tunnels compared to that observed in the case of a single tunnel.

Figure 8 and Table 3 show that the smallest normal forces induced in the preceding tunnel are obtained when the two tunnels are simultaneously excavated. An increase of lagging distance between the two tunnel faces is then followed by an increase in normal forces in the preceding tunnel all around the tunnel. The maximum normal forces are obtained when the lagging distance L_F reaches 2 or 3 times the shield length L_S. The increase of the lagging distance (i.e. $L_F = 8L_S$), however, causes a decrease in the normal forces of the preceding tunnel.

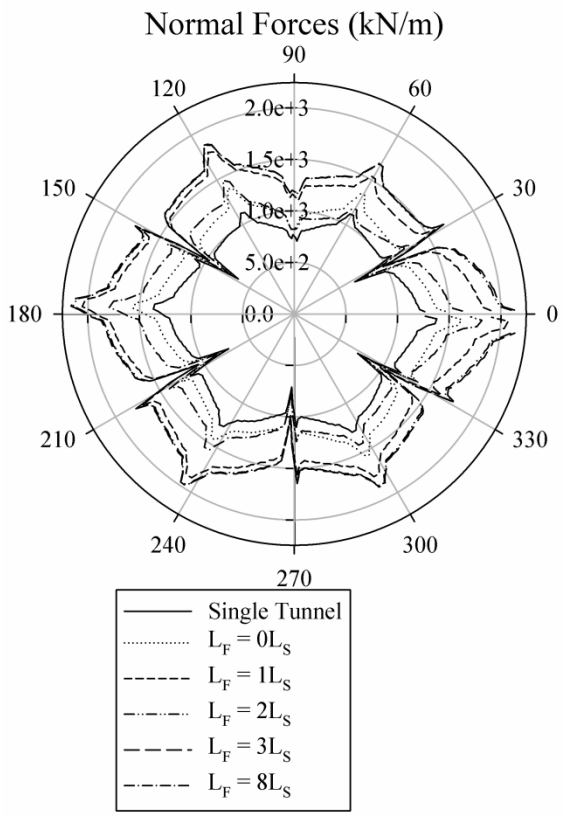

Figure 8. Normal forces induced in the lining of the preceding tunnel on the left.

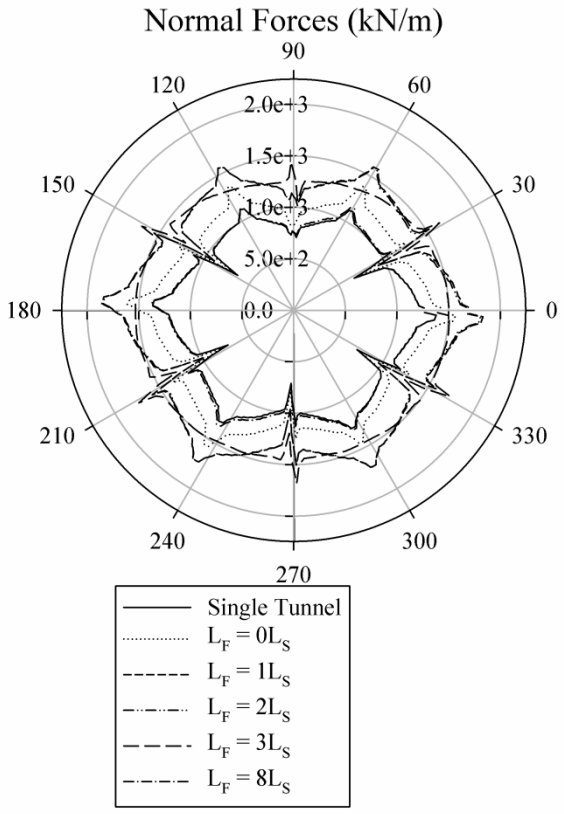

Figure 9. Normal forces induced in the lining of the following tunnel on the right.

As indicated by the numerical results obtained by the same authors [2] in the case of $L_F = 8L_S$ (or $10D_{tu}$), the advancing process of the following tunnel causes continuous change in the normal forces induced in the lining of the preceding tunnel. The maximum increase of the normal forces in the preceding tunnel is observed when the face of the following tunnel is across the measured lining section [2]. It should be mentioned that in this case the following tunnel is excavated when the lining in the preceding tunnel has reached a steady state. However, for the other cases of lagging distance considered in this study (i.e. $L_F = 1L_S$, $2L_S$, $3L_S$), the face of the following tunnel is across the measured lining section in the preceding tunnel when the structural forces in the preceding tunnel are still changing. It can be seen that the maximum change of the longitudinal forces in the preceding tunnel is observed when the lagging distance L_F is equal to $1L_S$, in particular at the right side near the following tunnel (Figure10). In this case, the face of the following tunnel is at the same transverse section as the tail of the shield machine of the preceding tunnel. At this location, the lining in the preceding tunnel is loaded by jacking forces at the shield tail. In addition, the cylindrical distribution pressures that act in the working chamber of the following tunnel cause the load transfer from this tunnel towards the preceding tunnel. The increase of the external loads in the radial direction causes an increase in the longitudinal forces in the lining of the preceding tunnel due to the partial restraint of the transversal deformation (Poisson effect) [2], as can be seen in Figure 10.

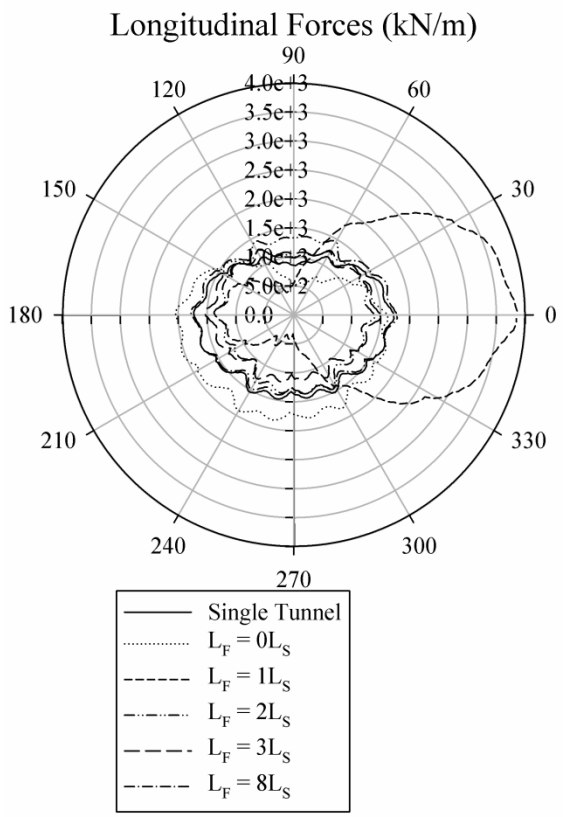

Figure 10. Longitudinal forces induced in the lining of the preceding tunnel on the left.

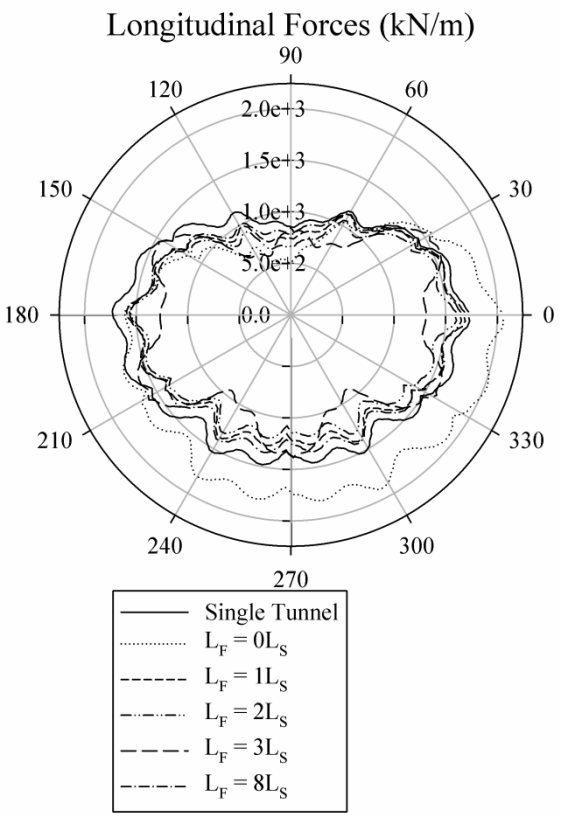

Figure 11. Longitudinal forces induced in the lining of the following tunnel on the right.

Figure 11 shows the longitudinal forces induced in the following tunnel. Unlike the preceding tunnel, the smallest normal forces induced in the following tunnel are observed when the lagging distance L_F is largest (i.e. L_F = 8 L_S) (see Table 4 and Figure 11). In this case the normal forces' values all around the tunnel are more or less similar to those induced in the case of a single tunnel (Figure 9). The same results have previously been obtained in the work of the same authors [2]. The normal forces in the tunnel lining when the lagging distance is L_F = 1L_S, 2L_S and 3L_S seem to be the same and reach the maximum values of about 135% compared to that of a single tunnel (Table 4). The normal forces in the case of the twin tunnels which are simultaneously excavated are in the middle. The increase of the normal forces induced in the following tunnel in the cases of L_F = 1L_S, 2L_S and 3L_S can be attributed to this tunnel being affected by the construction process of the preceding tunnel, such as grouting pressure at the shield tail. This grouting pressure causes the movement of the soil between the two tunnels toward the soil zone which the following tunnel will cross later. The additional outward displacement of the soil from the side of the following tunnel toward the following tunnel occurs at sections behind the shield tail where the grout has been hardened, which is also due to the effect of the small lateral earth pressure factor at rest (K_0 = 0.5). This movement leads to an increase of the external loads that act on the lining of the following tunnel. Consequently, the normal forces measured in the following tunnel are higher than those induced in a single tunnel.

Based on this, the explanation of why the small lagging distance leads to the higher normal forces in the following tunnel could be the smaller magnitude of the soil consolidation over the following tunnel caused by the excavation of the preceding tunnel. A larger downward movement over the following tunnel (see Table 4), and therefore of the external loads acting on the tunnel lining, is expected.

3.3. Bending moment in the tunnel lining

Figure 12 shows the distribution of the bending moment induced in the preceding tunnel on the left for different lagging distances between two tunnel faces. It can be seen that the excavation of two parallel tunnels generally causes an increase in the bending moment induced in the preceding tunnel, particularly on the right side near the following tunnel. This increase is really significant when the tunnels are excavated at a certain lagging distance. However, when the tunnels are simultaneously excavated, the bending moment induced in the preceding tunnel is more or less similar to that in a single tunnel (also see Table 3).

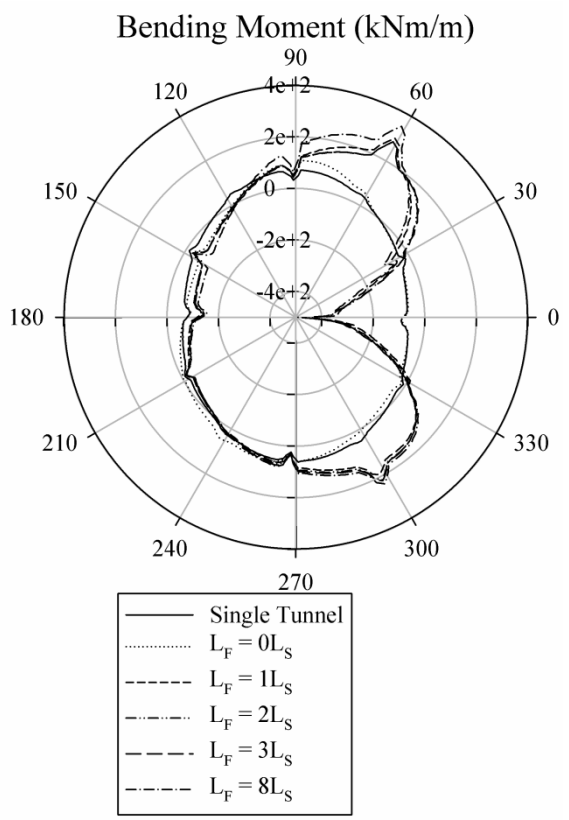

Figure 12. Bending moment induced in the lining of the preceding tunnel on the left.

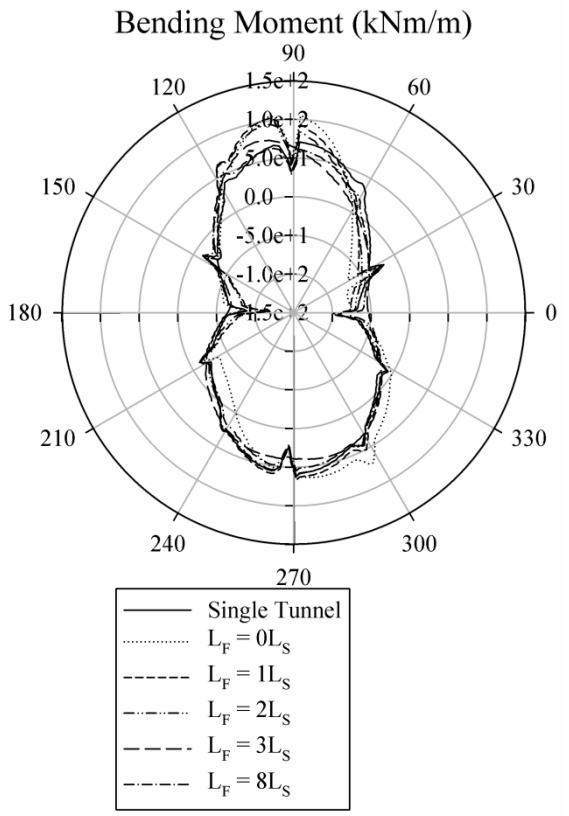

Figure 13. Bending moment induced in the lining of the following tunnel on the right.

The increase of the bending moment in the preceding tunnel in the case of lagging tunnels can be explained by the loss of the soil during the excavation of the following tunnel (see Do et al. [2]). The soil mass between the two tunnels has therefore a tendency to move towards the following tunnel. On the other hand, the soil above the preceding tunnel moves downwards. Consequently, an increase in the positive bending moment at the right shoulder and right base region and an increase in the absolute magnitude of the negative bending moment at the spring line are expected [2].

Figure 12 and Table 3 show that the maximum bending moment induced in the preceding tunnel is obtained when the lagging distance L_F is largest (i.e. $L_F = 8L_S$). The decrease of the lagging distance between tunnels is then followed by a decrease in the bending moment in the preceding tunnel. This could be attributed to the smaller downward movement of the soil above the preceding tunnel due to the effect of the following tunnel, as can be seen in Figure

6 and Table 3. The increase of the bending moment when the lagging distance between the tunnel faces increases also implies that the difference between vertical and horizontal loads increase, and therefore the ovalling loads around the following tunnel also increase.

Table 3. Development of the structural forces and deformation in measured ring 30 in the preceding tunnel on the left

Parameters	*Single tunnel*	*Lagging distance L_F (multiple of the length of shield machine L_S)*				
	-	*0*	*1*	*2*	*3*	*8*
Max. pos. bending moment (kNm/m)	71.9	109.9	297.2	278.3	278.4	348.1
R_{M+} (%)	*100*	*152.8*	*413.3*	*387.0*	*387.2*	*484.2*
Min. neg. bending moment (kNm/m)	-93.8	-97.4	-444.1	-492.7	-506.5	-480.6
R_{M-} (%)	*100*	*103.8*	*473.4*	*525.3*	*540.0*	*512.3*
Max. normal force (kN/m)	1490	1730	2232	2480	2518	1927
R_{N_max} (%)	*100*	*116.1*	*149.8*	*166.4*	*169.0*	*129.3*
Min. normal force (kN/m)	468	519.9	703.1	720.4	724.0	553.0
R_{N_min} (%)	*100*	*111.1*	*150.2*	*153.9*	*154.7*	*118.2*
Max. Longitudinal force (kN/m)	1745	2057	3888	1481	1554	1798
R_{LN} (%)	*100*	*117.9*	*222.8*	*84.9*	*89.1*	*103.1*
Max. normal displacement (mm)	5.69	9.4	11.8	12.6	13.1	15.4
R_{disp+} (%)	*100*	*165.0*	*206.5*	*221.6*	*230.5*	*271.0*
Min. normal displacement (mm)	-2.78	-4.7	-6.0	-7.0	-7.3	-8.6
R_{disp-} (%)	*100*	*170.6*	*217.1*	*252.6*	*264.3*	*311.0*
Max. surface settlement (mm)	-27.4	-43.8	-34.1	-33.7	-33.8	-40.3
R_{Sett-} (%)	*100.0*	*159.9*	*124.8*	*123.0*	*123.6*	*147.4*
Volume Loss Ratio (%) caused by the single preceding tunnel excavation			*0.92*			

Table 4. Development of the structural forces and deformation in measured ring 30 in the following tunnel on the right

Parameters	*Single tunnel*	*Lagging distance L_F (multiple of the length of shield machine L_S)*				
	-	*0*	*1*	*2*	*3*	*8*
Max. pos. bending moment (kNm/m)	71.9	109.1	105.7	97.5	77.6	65.8
R_{M+} (%)	*100*	*151.7*	*147.0*	*135.6*	*107.9*	*91.6*
Min. neg. bending moment (kNm/m)	-93.8	-94.5	-122.1	-114.9	-69.2	-89.9
R_{M-} (%)	*100*	*100.8*	*130.2*	*122.5*	*73.8*	*95.9*
Max. normal force (kN/m)	1490	1725	2016	2005	1981	1491
R_{N_max} (%)	*100*	*115.7*	*135.3*	*134.6*	*132.9*	*100.1*
Min. normal force (kN/m)	468	512.8	662.0	660.6	864.0	469.2
R_{N_min} (%)	*100*	*109.6*	*141.5*	*141.2*	*184.6*	*100.3*
Max. longitudinal force (kN/m)	1745	2074	1713	1630	1647	1667
R_{LN} (%)	*100*	*118.8*	*98.2*	*93.4*	*94.4*	*95.5*
Max. normal displacement (mm)	5.69	9.4	7.5	6.5	6.5	5.2
R_{disp+} (%)	*100*	*165.1*	*132.0*	*115.0*	*114.4*	*92.1*
Min. normal displacement (mm)	-2.78	-4.7	-3.3	-3.0	-3.0	-2.5
R_{disp-} (%)	*100*	*169.1*	*119.7*	*107.9*	*106.6*	*90.1*
Additional Volume Loss Ratio (%) caused by the following tunnel excavation	-	-	0.88	0.83	0.82	0.79
R_{VL} (%)	100	-	96.2	90.9	90.1	86.0
Total Volume Loss Ratio caused by the	-					

twin tunnel excavation (%)	1.81	1.80	1.75	1.74	1.71

Figure 13 shows the bending moment induced in the following tunnel on the right. Unlike the preceding tunnel, the higher the lagging distance between the tunnel faces, the smaller the maximum bending moment induced in the following tunnel (Figure 13 and Table 4). It should be mentioned that the interaction between the two tunnels causes higher effects on the bending moment at the top and at the left side of the following tunnel near the preceding tunnel (Figure 13). This could be explained by the decrease of the downward movement of the soil above the following tunnel when the lagging distance between tunnel faces is increased, as can be seen in Figure 7. Different from the preceding tunnel, the ovalling loads around the following tunnel decrease when the lagging distance L_F increases.

From the design point of view in terms of the lining stability, it is reasonable to note that the critical lagging distance between two tunnel faces is equal to L_S, where the face of the following tunnel is at the same transverse section as the shield tail of the preceding tunnel. Using this scenario, the lining stress state permits to determine the critical lagging distance.

4. CONCLUSIONS

In this study, a series of 3D numerical analyses of mechanized twin tunnels have been conducted, which has allowed the effect of the lagging distance along the tunnelling direction between tunnel faces on their structural behaviour and on the displacements of the ground surrounding the tunnels to be highlighted. On the basis of these 3D numerical analyses, it is possible to draw the following conclusions:

(1) The surface settlement trough over twin tunnels is strongly affected by the lagging distance L_F.
(2) The dependence of the downward movement over the preceding tunnel and over the following tunnel on the lagging distance L_F are opposite.
(3) The excavation of twin mechanized tunnels always causes an increase in the normal forces induced in the lining of both tunnels compared to that observed in the case of a single tunnel.
(4) The smallest normal forces induced in the preceding tunnel are obtained when the two tunnels are simultaneously excavated. However, this value is observed in the following tunnel when the lagging distance is large enough (i.e. $L_F = 8L_S$).
(5) The dependency of the maximum bending moment induced in the preceding tunnel and that in the following tunnel on the lagging distance L_F are opposite.
(6) The critical lagging distance between two tunnel faces in terms of the lining stability is equal to L_S, where the face of the following tunnel is at the same transverse section as the shield tail of the preceding tunnel.

In case of a mechanized twin tunnels excavation, the design study is then fundamental to investigate the excavation influence on the movements and the lining efforts.Experimental studies and on-site monitoring will also be necessary in the future to validate the numerical results obtained in this study.

References

[1] Do NA, Dias D, Oreste PP and Djeran-Maigre I. Two-dimensional numerical investigation of twin tunnel interaction. Geomechanics and Engineering 2013; 6(3): 263-275.
[2] Do NA, Dias D, Oreste PP and Djeran-Maigre I. Three-dimensional numerical simulation of a mechanized twin tunnels in soft ground. Tunnelling and Underground Space Technology 2014; 42:40-51.
[3] Do NA, Dias D, Oreste PP. 3D numerical investigation on the interaction between mechanized twin tunnels in soft ground. Environmental Earth Sciences 2014; 73(5): 2101-2113, doi: 10.1007/s12665-014-3561-6.
[4] Do NA, Dias D, Oreste PP. Three-dimensional numerical simulation of mechanized twin stacked tunnels in soft ground. Journal of Zhejiang University SCIENCE A 2014; 15(11), 896-913,doi: 10.1631/jzus.A1400117.
[5] Chapman DN, Ahn SK and Hunt DVL. Investigating ground movements caused by the construction of multiple tunnels in soft ground using laboratory model tests. Canadian Geotechnical Journal 2007; 44(6): 631-643.
[6] Choi JI and Lee S. Influence of existing tunnel on mechanical behaviour of new tunnel. KSCE Journal of Civil Engineering 2010; 14(5): 773-783.
[7] Ng CWW and Lu H. Effects of the construction sequence of twin tunnels at different depths on an existing pile. Canadian Geotechnical Journal 2014; 51: 173-183.
[8] Suwansawat S and Einstein HH. Describing settlement troughs over twin tunnels using a superposition technique. Journal of Geotechnical and Geoenvironmental Engineering 2007; 133(4): 445-468.
[9] Yang XL and Wang JM. Ground movement prediction for tunnels using simplified procedure. Tunnelling and Underground Space Technology 2011; 26: 462-471.
[10] Yamaguchi I, Yamazaki I and Kiritani Y. Study of ground-tunnel interactions of four shield tunnels driven in close proximity, in relation to design and construction of parallel shield tunnels. Tunnelling and Underground Space Technology 1998; 13(3): 289-304.
[11] Chen RP, Zhu J, Liu W and Tang XW. Ground movement induced by parallel EPB tunnels in silty soils. Tunnelling and Underground Space Technology 2011; 26: 163-171.
[12] Fang Q, Zhang D, Li QQ and Wong LNY. Effects of twin tunnels construction beneath existing shield-driven twin tunnels. Tunnelling and Underground Space Technology 2015; 45: 128-137.
[13] Nyren, R. Field measurements above twin tunnels in London Clay. PhD theses, Imperial College. 1998.
[14] Cording, E.J. and Hansmire, W.H. Displacement around soft tunnels. Proceedings 5th Pam-Am Conference on Soil Mechanics and Foundation Engineering, Buenos Aires 1975, Vol. 4, 571-633.
[15] Addenbrooke, T.I. Numerical analysis of tunnelling in stiff clay. PhD Theses, Imperial College, London 1996, p.373.
[16] Hage Chehade F and Shahrour I. Numerical analysis of the interaction between twin-tunnels: Influence of the relative position and construction procedure. Tunnelling and Underground Space Technology 2008; 23: 210-214.
[17] Hefny AM, Chua HC and Jhao J. Parametric studies on the interaction between existing and new bored tunnels. Tunnelling and Underground Space Technology 2004; 19: 471.
[18] Chakeri H, Hasanpour R, Hindistan MA and Ünver B. Analysis of interaction between tunnels in soft ground by 3D numerical modelling. Bull Eng Geol Environ. 2011; 70: 439-448.

[19] Channabasavaraj W and Vishwanath B. Influence of relative position of the tunnels: Numerical analysis on interaction between twin tunnels. Proceedings of Indian Geotechnical Conference 2012, Delhi, 500-503.
[20] Karakus M, Ozsan A and Basarir H. Finite element analysis for the twin metro tunnel constructed in Ankara Clay, Turkey. Bull Eng Geol Env. 2007; 66: 71-79.
[21] Zheng G, Zhang T and Diao Y. Mechanism and countermeasures of preceding tunnel distortion induced by succeeding EPBS tunnelling in close proximity. Computers and Geotechnics 2015; 66: 53-65.
[22] Ng CWW, Lee KM and Tang DKW. Three-dimensional numerical investigations of new Austrian tunnelling method (NATM) twin tunnel interactions. Cannadian Geotech. Journal 2004; 41: 523-539.
[23] Itasca Consulting Group. FLAC Fast Lagrangian Analysis of Continua, Version 4.0. User's manual, 2009.
[24] Do NA, Dias D, Oreste PP and Djeran-Maigre I. Three-dimensional numerical simulation for mechanized tunnelling in soft ground: The influence of the joint pattern. Acta Geotechnica 2013; 9(4): 673-694, doi 10.1007/s11440-013-0279-7.
[25] Do NA, Dias D, Oreste PP and Djeran-Maigre I. 2D numerical investigation of segmental tunnel lining behaviour. Tunnelling and Underground Space Technology 2013; 37: 115-127.
[26] Arnau O, & Molins C. Three dimensional structural response of segmental tunnel linings. Engineering Structures 2012; 44: 210-221.
[27] Addenbrooke, TI, and Potts, D M. Twin tunnel interaction surface and subsurface effects. International Journal of Geomechanics 2001, 1(2), 249-271

Highlights

- A strong effect of the lagging distance between mechanized tunnel faces on twin tunnels excavation has been highlighted;
- The tendency in the change of the bending moment and lining deformation in the preceding tunnel and the following tunnel depending on the lagging distance are generally opposite;
- The critical lagging distance between two tunnel faces in terms of the lining stability is equal to $1L_S$ where the face of the following tunnel is at the same transverse section with the shield tail of the preceding tunnel.